Subsonic Vortex-Flow Design Study for Slender Wings

John E. Lamar*
NASA Langley Research Center, Hampton, Va.

A theoretical study describing the effects of spanwise camber on the lift dependent drag of slender delta wings having leading-edge vortex flow is presented. The earlier work by Barsby, using conical flow, indicated that drag levels similar to those in attached flow could be obtained. This is re-examined and then extended to the more practical case of nonconical flow by application of the vortex-lattice method coupled with the suction analogy and the recently developed Boeing free-vortex-sheet method. Lastly, a design code is introduced which employs the suction analogy in an attempt to define "optimum" camber surfaces for minimum lift dependent drag for vortex flow conditions.

Nomenclature

A = aspect ratio
C_D = drag coefficient, $D/q_\infty S_{ref}$
$\Delta C_D/C_L{}^2$ = drag-due-to-lift parameter
C_L = lift coefficient, $L/q_\infty S_{ref}$
$C_{L,\,vortex}$ = lift coefficent contribution from vortex-flow aerodynamics
$C_{m|_{.3\bar{c}}}$ = pitching moment coefficient about $0.3\bar{c}$, $\dfrac{(\text{pitching moment})}{q_\infty S_{ref}\bar{c}}$
$C_{p,u}$ = pressure coefficient on upper surface, $\dfrac{(P_{upper}-P_{freestream\ static})}{q_\infty}$
ΔC_p = lifting pressure coefficient, $\dfrac{(P_{lower}-P_{upper})}{q_\infty}$
$\bar{c}$ = reference chord
D = drag
D_l = payoff function, $D+(k/2)(L-L_D)^2$
K_1 = $\dfrac{(\Delta C_D/C_L{}^2)_{vortex}}{(\Delta C_D/C_L{}^2)_{planar\ optimum}}$
K_2 = $\dfrac{(\Delta C_D/C_L{}^2)_{vortex}}{(\Delta C_D/C_L{}^2)_{nonplanar\ optimum}}$
K_3 = $\dfrac{(\Delta C_D/C_L{}^2)_{vortex}}{(\Delta C_D/C_L{}^2)_{attached}}$
k = factor in payoff function
L = lift
M = Mach number
$\bar{N}_c$ = number of horseshoe vortices in a chordwise row in vortex-lattice method
$\bar{N}_s$ = number of chordwise rows of horseshoe vortices in vortex-lattice method
P = pressure
p = nondimensional camber height for conically cambered wings in terms of local semispan
q_∞ = freestream dynamic pressure
RN = Reynolds number
S_{ref} = reference area
s = local semispan
U = freestream velocity
x/c = fractional distance along a local chord
x/c_r = fraction distance along the root chord
$2y/b(x)$ = fractional distance along the local semispan
z/c = local camber height in fractions of local chord
α = angle of attack
α_i = geometric incidence
α_l = local geometric angle of attack along camber line
α_{ll} = new local geometric angle of attack along camber line
Γ = local circulation
Λ = leading-edge sweep angle

Subscripts

attached = full leading-edge suction attached flow
D = design
vortex = total aerodynamic effect when vortex flow is present

Presented as Paper 78-154 at the AIAA 16th Aerospace Sciences Meeting, Huntsville, Ala., Jan. 16-18, 1978; submitted Feb. 14, 1978; revision received June 2, 1978.

Index categories: Aerodynamics; Computational Methods; Configuration Design.

*Aeronautical Research Scientist. Member AIAA.

Introduction

SLENDER wings have received attention and application primarily as supersonic cruise vehicles or research models of aircraft for the past 20 years. During this same time period, their use on fixed-sweep fighters has been limited because of the greater need for sufficient span and area to meet range and maneuver requirements coupled with generally only a supersonic dash capability. This was due primarily to the fighters being designed for standoff missile attack. However, more recently, there has been an increase of interest in the transonic maneuver part of the mission of a fighter as evidenced in the recent lightweight fighter competition. In particular, both airplanes employed leading-edge-vortex-lift strakes which provided a lightweight means of developing direct maneuver lift, as well as helping to stabilize the flow on the main wing at transonic maneuver conditions. It has been postulated that the next generation of fighters will retain the transonic maneuver requirement embodied in current aircraft as well as be able to cruise efficiently at supersonic speeds. This is the designated supercruise airplane. Therefore, it is likely that a slender wing will once again be employed, but this time having the additional requirement of maneuver.

The design of a slender wing for this multiple role is not well advanced. If one considers the use of maneuver flaps, they tend to be inefficient on slender wings, and, in addition to the variable geometry treatment required to maintain attached flow at the leading edge for high maneuver lift conditions, the deflections may be excessive. Another approach is to take advantage of the tendency of the leading-edge flow to separate and roll up into two conical-type vortices which generate the well-known vortex lift. However,

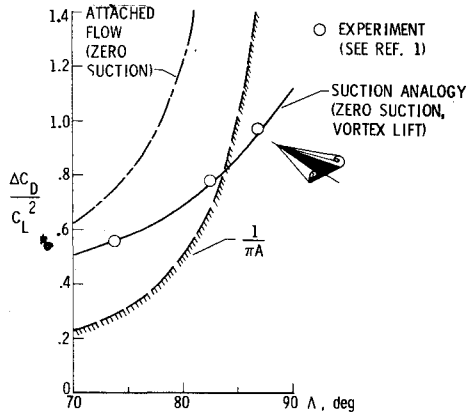

Fig. 1 Slender planar wing ($\Delta C_D/C_L{}^2$): $C_L = 0.3$, $M = 0.8$.

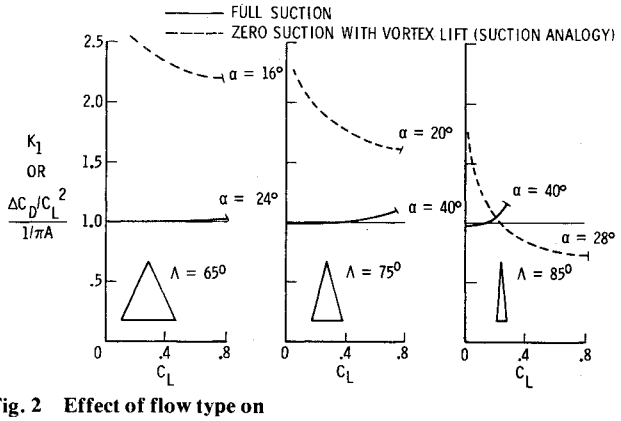

Fig. 2 Effect of flow type on $\frac{(\Delta C_D/C_L{}^2)}{(\Delta C_D/C_L{}^2)_{\text{planar optimum}}}$: $M = 0$, VLM $-\bar{N}_c = 8$, $\bar{N}_s = 25$.

if this vortex lift is to be generated efficiently, some means of shaping the wing to optimize the lift generated, while minimizing the drag associated with the loss of leading-edge suction, must be used. To accomplish this, it is necessary to either develop a general method which will determine the mean-camber shape by iteratively applying an analysis code under the control of an optimizing routine, or to go through the iteration procedure on a step-by-step basis under manual control.

The proposal to develop a wing with efficient vortex lift becomes a realistic goal as aspect ratio is reduced, since studies (see Ref. 1, for example) have indicated that on slender planar wings the lift dependent drag using vortex flow can be less than for attached flow. Figure 1 is taken from Ref. 1 and shows that for sweep angles larger than 83 deg measured drag-due-to-lift parameter values for wings with vortex flow are below that of $1/\pi A$ when $C_L = 0.3$ and $M = 0.8$. There are two explanations for this occurrence: 1) the leading-edge vortices act as fluid endplates; and 2) for slender wings not much leading-edge thrust is available to reduce the drag in attached flow, so it is better to let the the flow separate and reduce the angle of attack by additional flow entrainment to reach a particular C_L. This also shows up in reduced ΔC_D, because $\Delta C_D = C_L \tan\alpha$. The other two curves are for zero percent leading-edge suction. The upper curve is based on attached flow with no flow reattachment, Zero Leading-Edge Suction Attached Flow (ZLESAF), whereas the one labeled suction analogy, which agrees with the data, assumes that leading-edge vortices are formed, promoting the upper surface flow attachment and the development of vortex lift. The concept of the suction analogy was introduced for delta wings by Polhamus[2] and will be used herein as one of the theoretical methods.

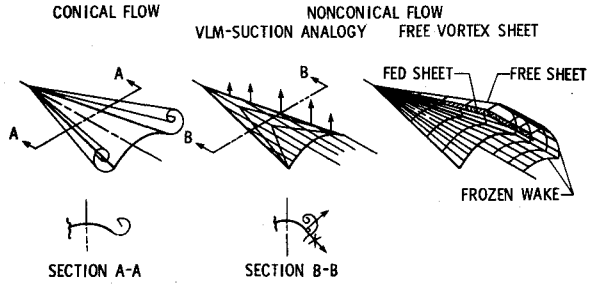

Fig. 3 Vortex-flow aerodynamic representation.

To get a clearer idea about how it is possible to obtain drag-due-to-lift parameters less than $1/\pi A$, Fig. 2 has been prepared. It shows solutions for the Full Leading-Edge Suction Attached Flow (FLESAF), including trigonometric terms, and the suction analogy for delta wings over a sweep range. Both solutions are computed from a modified version of the vortex-lattice method of Ref. 3. A study of the normalized curves, K_1 dicloses several interesting results: 1) the vertical separation between the two curves decreases with increasing C_L and Λ, and, in particular, the curves cross for $\Lambda = 85$ deg near $C_L = 0.2$; 2) for $\Lambda = 85$ deg, the solution from the suction analogy becomes lower than the FLESAF or the planar potential curves; 3) depending on sweep, the FLESAF solution differs only slightly from the planar potential result, at least over some C_L range; 4) at the higher sweeps, the maximum angle of attack used in the computations of $C_{L\max}$ is reached for the FLESAF solution before the C_L range is covered; and 5) at the higher sweeps and lower C_L values, a slight computational error is noted in that the FLESAF solutions are less than 1.

With the preceding background, the topic to be studied in this paper is the minimization of the drag-due-to-lift parameter in subsonic flow for slender delta wings having leading-edge flow separation with reattachment, or vortex flow. If the wings to be studied were restricted to planar ones, then it is obvious that with sufficient sweep this parameter can be made equal to or less than that of the planar optimum, and the study would be already concluded. However, as has been demonstrated, extremely large sweep angles are required in order to accomplish this task, resulting in aspect ratios of 0.5 or less. Wings in this aspect ratio range are not practical from an aircraft range/payload viewpoint; thus, improvements in the drag-due-to-lift parameter for wings with lower sweep are sought. Therefore, mostly nonplanar wings of delta planform will be examined in this theoretical study. The nonplanar variation will be restricted to conical camber with the realization that this camber will most likely not be optimum. Hence, in an attempt to establish an optimum shape, a new computer code which incorporates the suction analogy has been developed and a preliminary solution is given.

Theoretical Methods Used

The analytical study will employ three different theoretical methods, one conical and two nonconical. They are 1) the conical flow method of Smith[4] or Barsby,[5] 2) Vortex-Lattice-Method with Suction Analogy (VLM-SA),[3] and 3) Boeing free-vortex sheet.[6] These methods, depicted in idealized form by Fig. 3, differ in several ways, among them are Kutta condition satisfaction, Mach number dependence, and separated flow modeling. The conical flow and free-vortex-sheet methods model the separated-flow vortex sheet and satisfy the leading-edge Kutta condition, but only the VLM-SA and free-vortex-sheet methods satisfy the trailing-edge Kutta condition. The conical flow solution has no Mach number dependence because of its underlying assumption, i.e., $M \approx 1$, which is reasonable for very slender wings; whereas, the nonconical flow methods both have Mach number dependent terms. However, since this study is

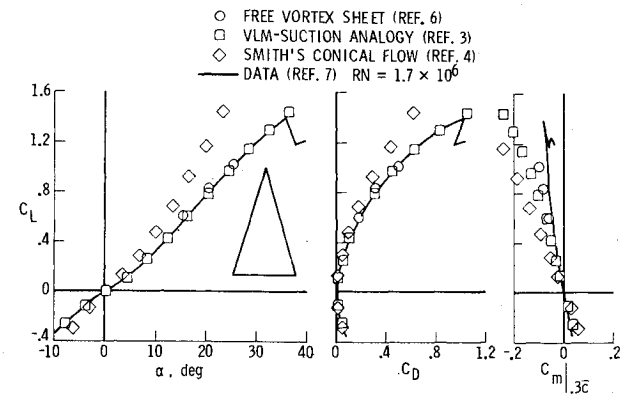

Fig. 4 Longitudinal aerodynamic results for 74-deg planar delta wing, $M \approx 0$.

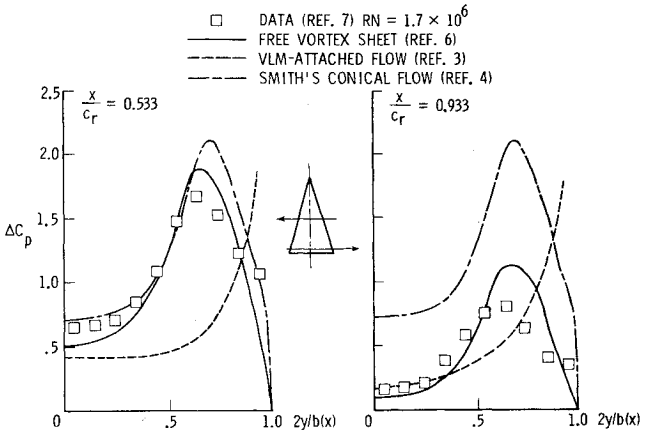

Fig. 5 Spanwise pressure distribution for 74-deg planar delta wing, $\alpha = 20$ deg, $M \approx 0$.

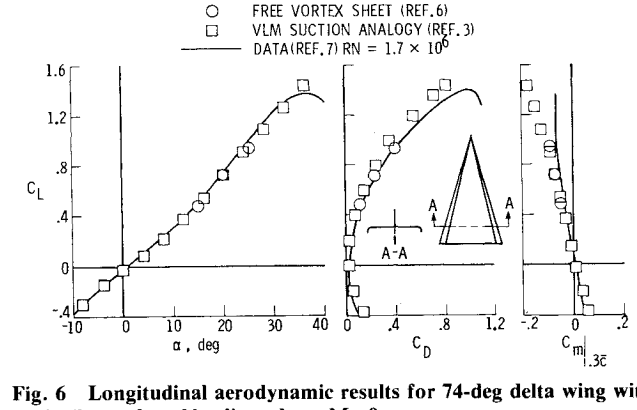

Fig. 6 Longitudinal aerodynamic results for 74-deg delta wing with conically cambered leading edges, $M \approx 0$.

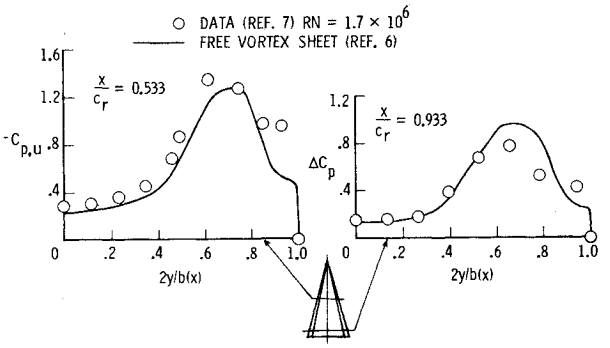

Fig. 7 Spanwise pressure distributions for 74-deg delta with conically cambered leading edges, $\alpha = 20$ deg, $M \approx 0$.

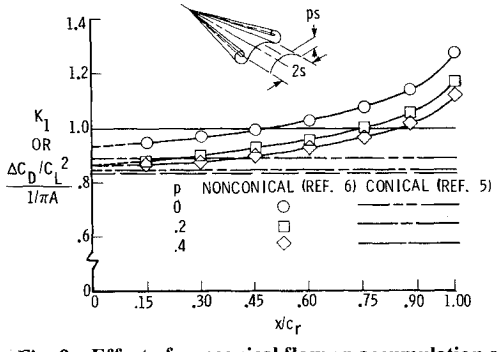

Fig. 8 Effect of nonconical flow on accumulation of $\dfrac{(\Delta C_D/C_L{}^2)_{\text{vortex}}}{(\Delta C_D/C_L{}^2)_{\text{planar optimum}}}$: $\Lambda = 80$ deg, $M = 0$.

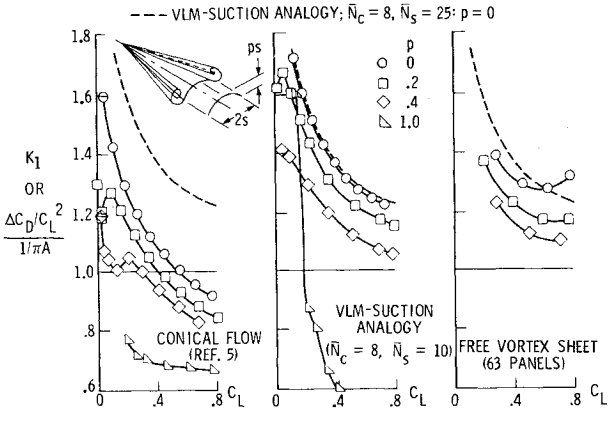

Fig. 9 Effect of camber height on $\dfrac{(\Delta C_D/C_L{}^2)_{\text{vortex}}}{(\Delta C_D/C_L{}^2)_{\text{planar optimum}}}$: $\Lambda = 80$-deg delta wing, $M = 0$.

primarily for slender wings, where the effects of Mach number will be small, all calculations for the nonconical methods will be done at a Mach number equal to zero.

To obtain an understanding of the accuracy of these methods, they are compared in Figs. 4-7 with two sets of experimental data from Ref. 7. (Note that Fig. 5 was essentially taken from Ref. 8.) The first set of data is for a planar 74-deg delta wing, and the second set is for a 74-deg delta wing with conically cambered leading edges. The following conclusions are drawn from a study of these figures: 1) VLM-SA gives the best overall estimate of C_L vs α; 2) the free-vortex-sheet method predicts the C_D vs C_L better than the VLM-SA for the conically cambered wing; 3) the free-vortex-sheet method estimates the C_m vs C_L as good as or better than the VLM-SA; 4) both the free-vortex-sheet method and VLM-SA predict the overall aerodynamic characteristics better than does the conical flow method; and 5) the free-vortex-sheet method predicts the experimental spanwise pressure distributions best of all three methods though not as well as might be expected from overall results. The free-vortex-sheet method, therefore, represents an improvement in pressure estimation; but, there is still room for improvement in the singularity representation and flow modeling.

As an aside, but related to the behavior of the flow, it is often stated that conical flow should give a reasonable estimate of the aerodynamic characteristics on the forward part of a delta wing where the trailing-edge effects are minimized. To explore the degree to which this holds, Fig. 8

has been prepared, which shows, for a range of conical camber heights, the nonconical flow effects on the accumulated K_I referenced by the accumulated area. Based on the free-vortex-sheet method, the result is that practical departures from conical flow extend all the way to the wing apex for all p values examined.

It should be noted that the effect of increasing p on K_I is seen to produce similar results with either method. Also, the free-vortex-sheet produces an accumulation of $K_I > 1$ for all values of p, at $x/c_r = 1$, whereas the accumulations from conical flow do not change and remain < 1 with increasing x/c_r because of the inherent assumptions.

Study of Drag-Due-to-Lift Parameter

The drag-due-to-lift parameters normalized by the planar potential result, K_I, for an 80-deg delta wing are presented in Fig. 9 for all three theoretical methods as a function of conical camber height and C_L. The range of p to be covered was 0 to 1.0 but, solutions from the free-vortex-sheet method did not converge at any α examined for $p = 0.6$ or 1.0. Hence, only solutions for p of 0.2 and 0.4 are presented for this method. The other two methods could compute K_I for both $p = 0.6$ and 1.0, but only the latter is graphed to reduce the amount of information presented.

To assist in gaging the accuracy of the K_I predictions from the three methods, the VLM-SA at $\bar{N}_c = 8$ and $\bar{N}_s = 25$ is offered as a reference curve for $p = 0$. This method was chosen because it estimated very well the planar wing C_L and C_D data of Fig. 4. Upon comparing the three methods with the reference curve, it can be seen that: 1) the conical flow results are much less, as would be expected from Fig. 4 where the estimates for C_L are high and C_D are low; 2) using $\bar{N}_s = 10$ instead of $\bar{N}_s = 25$ in the VLM-SA, because of the limited number of line segments which are available to model the conical camber for $p > 0$, consequently employed at $p = 0$ for consistency, leads to only small error, which grows slightly with increasing C_L; and 3) the free-vortex-sheet curve has a different variation than the reference curve over the indicated C_L range and reaches a minimum that is higher and occurs at a lower C_L than that of the reference curve; the minimum of which is not shown.

With an assessment of the accuracy of the three methods completed, an examination of the overall variation of K_I with p and C_L is made, which shows that for all these methods K_I generally decreases as either or both p or C_L is increased. To assess the effect that anhedral has on these results, the nonplanar optimum solutions of Cone[9] are used to nondimensionalize the $(\Delta C_D/C_L{}^2)_{\text{vortex}}$ values and the results designated as K_2 on Fig. 10.

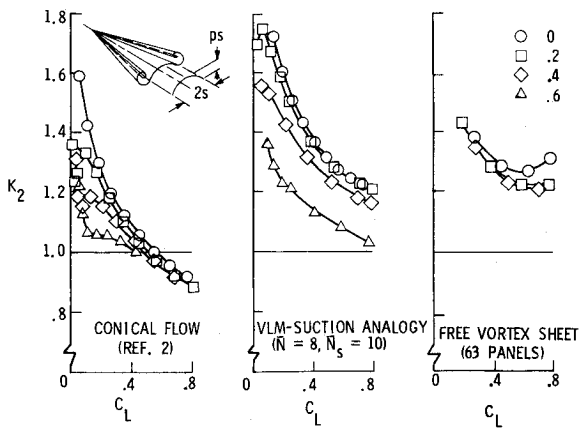

Fig. 10 Effect of camber height on

$$\frac{(\Delta C_D/C_L{}^2)_{\text{vortex}}}{(\Delta C_D/C_L{}^2)_{\text{nonplanar optimum}}}$$

: $\Lambda = 80$-deg delta wing, $M = 0$.

The K_2 values in this figure have the same general trends as before, but with a reduction in the vertical separation from the $p = 0$ solutions. Note, in particular, that it is necessary to reach a higher C_L value before it is beneficial to let the flow separate, i.e., before $K_2 \leq 1$. The conclusion from this figure is that there is a benefit to be gained by letting the flow separate on a conically cambered delta wing if p or C_L is large enough. Also, note that the VLM-SA $p = 1.0$ solution does not appear here, but instead, that of $p = 0.6$. This is because on Fig. 9 there was indication that a limit in the method to handle large anhedral angles in combination with large twists/cambers had been reached. The $p = 0.6$ results appear more reasonable; however, they are not used subsequently since they tend to suggest a lower useful bound for this method.

Based on the accuracy study and general trends of the methods, it was decided to proceed with one method, that being the VLM-SA, and a p range from 0 to 0.4 for the remainder of this part of the study. This method performs the computations with the same order of simplicity and cost as the conical flow solution, but with comparable accuracy and two orders-of-magnitude lower cost than the free-vortex-sheet method. On the left of Fig. 11 is repeated the K_2 curves of Fig. 10 as one part of the effect of wing geometry on K_2. A crossplot of K_2 from Fig. 10 as a function of p for three different C_L values is given in the middle of Fig. 11 and shows more clearly the reduction which takes place by increasing p. At the right is shown the effect of increasing leading-edge sweep at $p = 0.2$ for three different C_L values. Just as for the planar wings of Fig. 2, increasing sweep reduces K_I or K_2 at a fixed C_L. Similar results are obtained for variations of K_3, the vortex-flow drag-due-to-lift normalized by the solution for FLESAF.

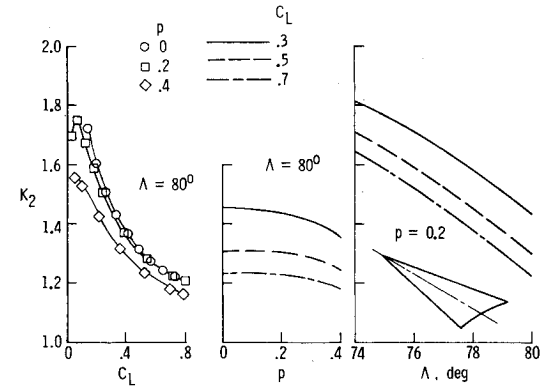

Fig. 11 Effect of delta wing geometry on

$$\frac{(\Delta C_D/C_L{}^2)_{\text{vortex}}}{(\Delta C_D/C_L{}^2)_{\text{nonplanar optimum}}}$$

: $M = 0$, VLM-SA – $\bar{N}_c = 8$, $\bar{N}_s = 10$.

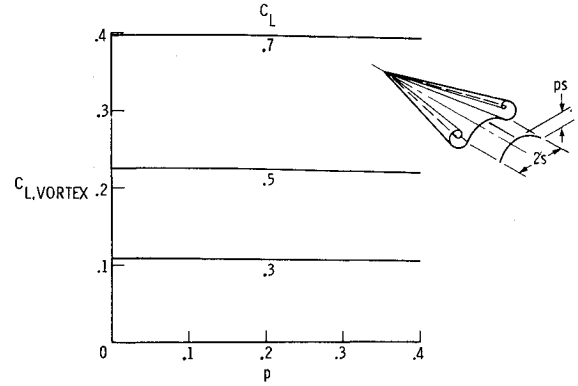

Fig. 12 Effect of p and C_L on $C_{L,\text{vortex}}$: $\Lambda = 80$ deg, $M = 0$, VLM-SA – $\bar{N}_c = 8$, $\bar{N}_s = 10$.

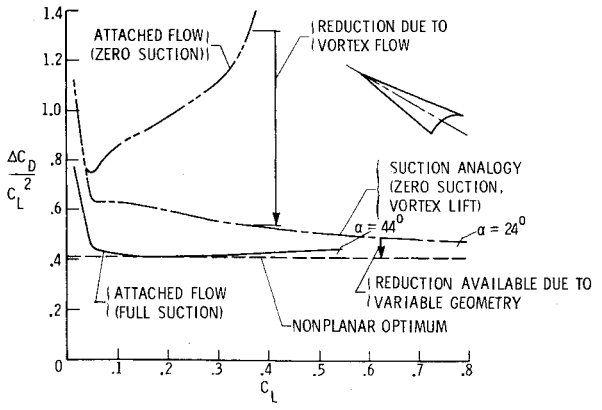

Fig. 13 Effect of flow type on $\Delta C_D/C_L{}^2$: $\Lambda = 80$ deg, $p = 0.4$, $M = 0$, VLM – $\bar{N}_c = 8$, $\bar{N}_s = 10$.

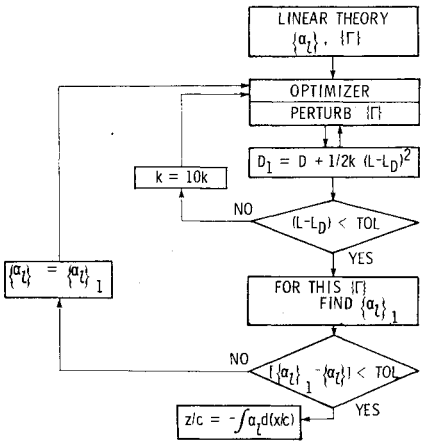

Fig. 14 Flow chart of vortex-flow wing design VLM for drag minimization with lift constraint.

One concern that might be present with regard to using the VLM-SA, herein, is that it concentrates the vortex-flow force at the leading edge and uses the local camber slope at the leading edge to determine the force and moment contributions. This is of special interest with regard to the drag estimation in that the result might be optimistic. Figure 12 has been prepared to study this problem indirectly, in that it is possible with increasing p for the local camber and twist specifications to suppress the leading-edge suction, and, therefore, the vortex lift. Suppressing this lift could give the reductions noted in K_1 and K_2 by causing the flow to be more nearly like a smooth-onflow solution in which the suction is carried distributively and the $C_{L,D}$ is large. Figure 12, shows, however, that with increasing p the $C_{L,\text{VORTEX}}$ is essentially a constant fraction of the total C_L for each C_L graphed, due to the slight increase in angle of attack required. Thus, the mean camber surfaces associated with an increasing p for conical camber are no more associated with smooth onflow than for the planar wing, $p = 0$, and the reduction in K_1 or K_2 that takes place is the result of the vortex-flow aerodynamics rather than being associated with a reduction of them.

Figure 13 is a summary figure of the drag-due-to-lift parameter variation with C_L for an 80-deg delta wing at $p = 0.4$ and includes solutions due to two attached flows and one vortex flow. This figure presents several interesting pieces of information: 1) for FLESAF the $(\Delta C_D/C_L{}^2)$ is almost the same as the nonplanar optimum at $C_L \approx 0.2$ even though the former is from a near-field solution; 2) for ZLESAF the $(\Delta C_D/C_L{}^2)$ reaches a minimum of about twice that of the nonplanar optimum and its curve exceeds a value of 1.4 for $\alpha > 30$ deg; 3) if one thinks in terms of going from the FLESAF curve to the ZLESAF curve when the leading-edge force is lost, it is important to realize that for thin wings with high sweep the flow will form vortices so the change will be only from the FLESAF to the suction-analogy curve (thus, the vortex formation provides a natural means of reducing $\Delta C_D/C_L{}^2$ and yields only a small fraction of the anticipated increase); 4) the $\Delta C_D/C_L{}^2$ associated with vortex flow, from the suction-analogy solution, continues to decrease over the α range, whereas the FLESAF solution result increases after its minimum is reached; 5) due to the action of the vortex flow much lower angles of attack are required to reach a given C_L and, in fact, it is possible for this fixed geometry with FLESAF to reach C_L levels much larger than shown, since its $C_{L,\max}$ is 0.597; and 6) the improvement in $\Delta C_D/C_L{}^2$ which may be gained by keeping the flow at the nonplanar optimum is difficult over the C_L range because of the tendency of the flow to separate. However, if variable geometry devices were added, primarily near the leading edge, the reduction available in $\Delta C_D/C_L{}^2$ would be the increment indicated from the suction-analogy curve. Thus, there is an α range with vortex flow in which the increase in $\Delta C_D/C_L{}^2$ from the nonplanar optimum is small even though the C_L range is vastly extended from that of the FLESAF. Considering this fact and recognizing the extreme difficulty and weight penalty associated with attempting to keep the flow attached, it may be best to let the flow separate in the maneuver and utilize vortex lift.

Vortex Flow Wing Design Using Suction Analogy

This section describes a procedure by which a first effort is made in using the suction analogy to design the mean-camber surface of a wing which is to have leading-edge vortex flow. The resulting design represents an optimum shape for the assumptions employed just as the attached-smooth-onflow solution does and should, therefore, yield values of $\Delta C_D/C_L{}^2$ near the planar or nonplanar optimum, depending on the wing geometry, just as the attached-flow solution does. The approach to be used is based on the idea that the vortex-flow mean-camber shapes represent small deviations from an attached-smooth-onflow solution, so that the vortex does not become large, which enables the suction analogy to be employed. Therefore, the techniques used are 1) the attached-smooth-onflow design code of Ref. 10, based on the VLM, which is employed to obtain a starting solution, and 2) the lift and drag equations from the VLM-SA which include nonlinear contributions from the circulation in addition to trigonometric terms involving α and the local angle of attack due to camber/twist, α_l.

An expected limitation of this procedure is the same as for the VLM-SA; that is, the vortex generated is assumed to remain small and near the leading edge. Deviations from this size and location will cause a degradation in $\Delta C_D/C_L{}^2$ thereby making the computed results optimistic.

An outline or flow chart of the vortex-flow design code is given on Fig. 14. It should be noted that this design method is an iterative one and not a direct solution as in the attached-flow solution. The outlined solution steps are as follows: 1) determine $\{\alpha_l\}$ and $\{\Gamma\}$ from the linear theory[10]; 2) enter the CONMIN optimizer[11] with $\{\alpha_l\}$ and $\{\Gamma\}$ and perturb each term in the $\{\Gamma\}$; 3) with the perturbed $\{\Gamma\}$ compute the payoff function D_1 in terms of the lift and drag developed, L and D, respectively; 4) repeat for each perturbed $\{\Gamma\}$ set and then optimize so as to minimize D_1; 5) with the $\{\Gamma\}$ that minimizes D_1 determine if it satisfies the lift constraint to within a tolerance; 6) if not, change the scaling k by a factor of 10 and begin repeating with step 2; 7) if so, determine from linear theory the $\{\alpha_l\}$ called $\{\alpha_l\}_1$, compatible with the $\{\Gamma\}$; 8) compare the $\{\alpha_l\}_1$ with the original $\{\alpha_l\}$ to determine if each term is within a tolerance; 9) if not, make $\{\alpha_l\} = \{\alpha_l\}_1$ and repeat from step 2; and 10) if so, then integrate using a spline routine the α_l's associated with a particular spanwise position from the trailing edge forward to determine the local

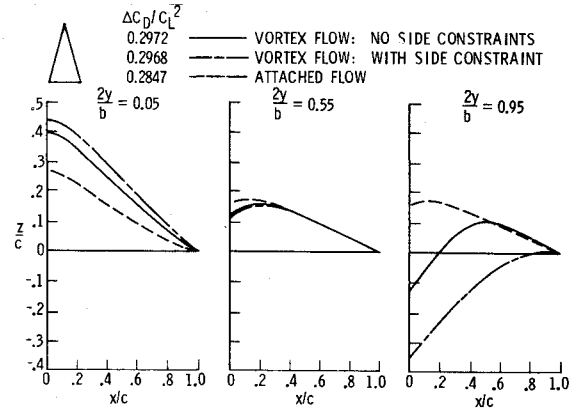

Fig. 15 Mean-camber shapes designed from vortex flow (suction analogy): $\Lambda = 75$ deg, $C_{L,D} = 0.3$, $M = 0$, $\bar{N}_c = 20$, $\bar{N}_s = 10$, $1/\pi A = 0.2970$.

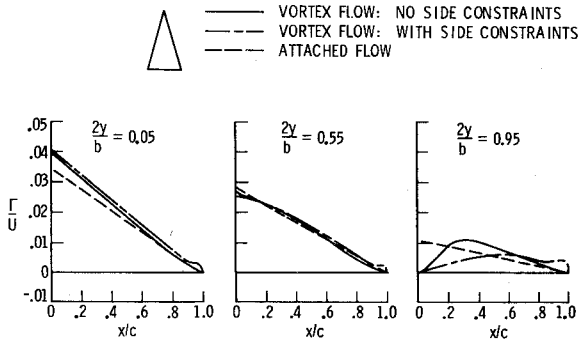

Fig. 16 Chord loadings from vortex-flow (suction analogy) design: $\Lambda = 75$ deg, $C_{L,D} = 0.3$, $M = 0$, $\bar{N}_c = 20$, $\bar{N}_s = 10$.

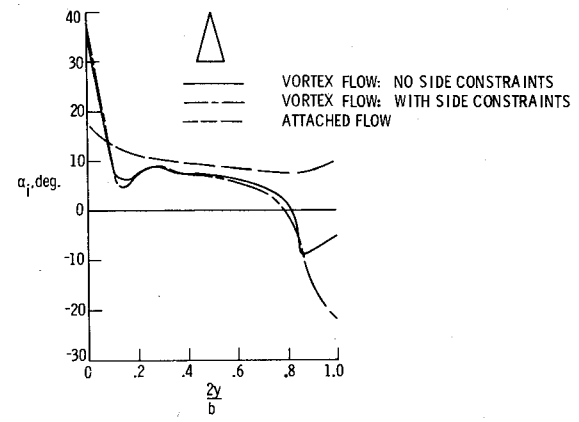

Fig. 17 Incidence distribution from vortex-flow (suction analogy) design: $\Lambda = 75$ deg, $C_{L,D} = 0.3$, $M = 0$, $\bar{N}_c = 20$, $\bar{N}_s = 10$.

elevations along the chord, i.e., mean-camber lines. Repeat at each spanwise position then stop. This entire procedure for the example wing with 200 panels requires nine iterations on $\{\Gamma\}$ and six iterations on $\{\alpha_l\}$ and is accomplished in about 400 central processing seconds on the CDC CYBER 175 digital computer.

Examples of the results of this procedure are given in Figs. 15-17 for a 75-deg planar delta wing at a $C_{L,D} = 0.3$ and $M = 0$. There are three sets of curves presented. Two are vortex-flow solutions with and without any constraints on the minimum levels of $\{\Gamma\}$, called side constraints, and other is the attached-smooth-onflow solution, given for reference.

The detail results for the three solutions on Figs. 15-17 will be discussed together. The only other item to be discussed is found on Fig. 16 where the drag-due-to-lift parameters for the two vortex-flow solutions are seen to agree well with the planar optimum result of 0.2970. However, just as in Ref. 12 for low-aspect-ratio wings and small $\bar{N}_c$ values, the results from the attached-flow solution is slightly low with respect to the planar optimum. Examining the three figures, it is obvious that both vortex-flow solutions lead to higher incidence angles inboard and less outboard; therefore, more twist is imposed. There appear to be two reasons for this occurrence. The first is to build up the loading (Γ/U) inboard and, consequently, the vortex lift in a region where the planar vortex lift is typically small. The second is that outboard, where the planar vortex lift would be high, it is suppressed somewhat so that a ramplike mean-camber line can be generated. This camber line and the one near midsemispan are so shaped as to allow the vortex flow that develops near the leading edge to generate a force component which can reduce the drag. The effect of imposing a constraint to keep the local lift positive, called side constraint and assured by keeping $(\Gamma/U) > 0$, is most noticed on the outermost 20% of the wing, especially near the wing tip, where, in order to keep $(\Gamma/U) > 0$ near the leading edge, the chord load and camber line are considerably altered.

There are two general observations which need to be made about the presented results. 1) Even though chord loadings (Γ/U) are graphed for the attached- and vortex-flow solutions, it should be understood that the suction pressures associated with the separated vortex are not modeled. They are only accounted for in an overall manner through the suction analogy, which leads to an estimate of the vortex-flow aerodynamic results. 2) Vortex-flow mean-camber lines do differ by more than a small amount, except at midsemispan, from the attached-flow solutions. This possibility was not anticipated and could, therefore, impact on the effectiveness of the resulting wing. However, regardless of the final camber design, only by model construction and wind-tunnel testing will an assessment be possible of this vortex-flow design procedure.

Conclusions

With regard to reducing the drag-due-to-lift parameter for slender delta wings having vortex flow, the present study is split into two parts. The first part deals with analytical methods and their application in the study of pertinent geometrical parameters. The second part deals with an initial attempt to define the mean-camber surface of a delta wing with vortex flow by using the suction analogy.

Part one is based on the results of the study using three different theoretical methods, i.e., conical flow, vortex-lattice with suction analogy and free-vortex-sheet, and geometry variations of conical-camber height and leading-edge sweep. It yielded the following conclusions.

1) In comparison to the other two theoretical methods, the vortex-lattice method with suction analogy (VLM-SA) predicts reasonable trends of the vortex-flow drag-due-to-lift parameter for conical-camber height and leading-edge-sweep variations. This method does so with a simplicity and cost of the same order of magnitude as conical flow solutions, but with comparable accuracy and with two orders-of-magnitude lower cost than the free-vortex-sheet method. The VLM-SA is used subsequently.

2) The drag-due-to-lift parameter is, in general, reduced by increasing lift coefficient, conical-camber height or leading-edge sweep.

3) The reduction in vortex-flow drag-due-to-lift parameter with increasing lift coefficient or camber height is not due to the wing approaching an attached-flow design point, but because the vortex-flow lift has a steeper forward facing slope to act over and thereby gives an effective thrust. While it is true that the twist and camber of the conically cambered delta wings increase with conical height, even more twist and camber are required to bring the flow to a near smooth-onflow situation.

4) For slender concially cambered delta wings, vortex flow provides a simple, natural way to reduce the drag-due-to-lift parameter over a wide range of lift coefficients if the edge force is lost and also provides a simple method of maintaining levels of this parameter near that of the full leading-edge-suction attached-flow solution at moderate lift coefficients.

5) Also for these wings, the available improvement in the drag-due-to-lift parameter in terms of the increment between the vortex-flow curve and the nonplanar optimum is small at the higher lift coefficients and would probably negate the use of variable geometry devices required to keep the flow attached with smooth onflow. Also, if such devices were used, there would be an associated weight penalty.

The second part of this drag-due-to-lift parameter study was concentrated on an initial attempt to define a mean-camber surface which would be optimum within the constraint of using the suction analogy to model (in an overall sense) the vortex-flow effects. The procedure was outlined and a 75-deg delta wing was used as an example. It was found that the vortex-flow camber-heights were higher inboard and lower outboard than the attached-smooth-onflow solutions, thereby yielding a larger twist requirement. The resulting drag-due-to-lift parameters for the vortex-flow solutions were the same as for the planar optimum.

References

[1] Polhamus, E. C., "Subsonic and Transonic Aerodynamic Research," *Vehicle Technology for Civil Aviation,* NASA SP-292, 1971, pp. 27-44.

[2] Polhamus, E. C., "A Concept of the Vortex Lift of Sharp-Edge Delta Wings Based on a Leading Edge Suction Analogy," NASA TN D-3767, 1966.

[3] Lamar, J. E. and Gloss, B. B., "Subsonic Aerodynamic Characteristics of Interacting Lifting Surfaces with Separated Flow Around Sharp Edges Predicted by a Vortex-Lattice Method," NASA TN D-7921, 1975.

[4] Smith, J. H. B., "Improved Calculations of Leading-Edge Separation from Slender Delta Wings," Royal Aircraft Establishment, Technical Rept. No. 66070, March 1966.

[5] Barsby, J. E., "Flow Past Conically Cambered Slender Delta Wings with Leading-Edge Separation," Aeronautical Research Council Reports and Memoranda No. 3748, 1974.

[6] Weber, J. A., Brune, G. W., Johnson, F. T., Lu, P., and Rubbert, P. E., "A Three-Dimensional Solution of Flows Over Wings with Leading-Edge Vortex Separation," AIAA Paper 75-866, Hartford, Conn., June 16-18, 1975.

[7] Wentz, W. H. Jr., "Effects of Leading-Edge Camber on Low-Speed Characterisitcs of Slender Delta Wings,"NASA CR-2002, 1972.

[8] Kuhlman, J., "Load Distributions on Slender Data Wings Having Vortex Flow," *Journal of Aircraft,* Vol. 14, July 1977, pp. 699-702.

[9] Cone, C. D. Jr., "The Aerodynamic Design of Wings with Cambered Span Having Minimum Induced Drag," NASA TR-R-152, 1963.

[10] Lamar, J. E., "A Vortex-Lattice Method for the Mean Camber Shapes of Trimmed Noncoplanar Planforms with Minimum Vortex Drag," NASA TN D-8090, 1976.

[11] Vanderplaats, G. N., "CONMIN-A Fortran Program for Constrained Function Minimization – User's Manual, " NASA TM X-62282, 1973.

[12] Margason, R. J., and Lamar, J. E., "Vortex-Lattice Fortran Program for Estimating Subsonic Aerodynamic Characteristics of Complex Planforms," NASA TN D-6142, 1971.